A diffuse multipath spectrum estimation technique for directional channel modeling

Jon Wallace*, Hüseyin Özcelik†, Markus Herdin†, Ernst Bonek†, and Michael Jensen*

*Department of Electrical and Computer Engineering
Brigham Young University, 459 CB, Provo, UT 84602-4099
Phone: (801)422-5736 Fax: (801)422-0201
Email: jensen@ee.byu.edu

†Institut für Nachrichtentechnik und Hochfrequenztechnik
Technische Universität Wien, Gusshausstrasse 25/389, A-1040 Wien, Austria
Phone: (+43 1) 58801 - 38901 Fax: (+43 1) 58801 - 38999
Email: ernst.bonek@tuwien.ac.at

***Abstract*— A diffuse spectrum estimation method is presented that is suitable for direction finding for channels with diffuse electromagnetic scattering. The diffuse channel may be the result of physical phenomena (e.g., rough-surface scattering) or limited angular and temporal discrimination of the channel probing equipment. The method decomposes the ideal non-coherent spectrum into a sum of power-weighted basis functions. The basis function coefficients are obtained through a linear programming solution. The method is applied to recent radio channel data collected on the Vienna University of Technology campus. Parameters for a path-based model are extracted using the technique. Site-specific spectra and global capacity comparisons indicate the utility of this new method.**

I. Introduction

The double-directional channel concept has emerged as a powerful system-independent representation of point-to-point wireless channels [1]. When the channel is correctly characterized by the double-directional transfer function, the response of the channel for arbitrary antenna arrays may then be computed. In previous work, the double-directional channel has been assumed to consist of a discrete sum of plane waves, referred to herein as the *specular* assumption. In this case, parametric techniques such as ESPRIT [2], [3] can be used to jointly compute direction of departure (DOD) and direction of arrival (DOA) for each multipath component.

Unfortunately, methods assuming specular scattering break down in environments that are inherently *diffuse*. A diffuse channel may result from physical scattering phenomena, such as rough-surface scattering. In very rich scattering environments, the number of multipath components may be too large to be individually resolved by the finite number of antennas and frequency samples, leading to a quasi-diffuse channel, regardless of the underlying scattering mechanism. In diffuse environments, conventional beamforming techniques may be employed [3], yielding a continuous spectrum for the directional channel response. For double-directional probing, a joint spectrum is appropriate [4]. DOAs and DODs then loosely correspond to the peaks of the joint spectrum. However, such methods are somewhat problematic from a double-directional modeling perspective, since the continuous joint spectrum represents an infinite set of parameters.

In this work, we present a new estimation technique that represents the directional channel response as a set of arbitrary basis functions. These basis functions correspond roughly to *clusters* of multipath departures/arrivals, where each multipath component cannot be identified individually. We show that when the underlying functional form of the the clusters is known, the method identifies DOD/DOA and cluster angular spread with high accuracy. The method fits well with the double-directional concept, since the channel is represented by a small set of parameters, i.e. cluster shape, DOA/DOD, and cluster angular spread. The method is general and applicable to arbitrary transmit and receive arrays. Finally, due to the natural compatibility with multipath cluster models, such as the Saleh-Valenzuela angular (SVA) model [5], [6], the method allows model parameters to be computed from data and realistic channel covariance matrices to be generated synthetically.

II. Conventional Directional Estimation

Consider a very rich scattering environment where multipath components arrive in Laplacian-shaped clusters with 15° angular spread. The channel is probed with a single omni-directional transmitter. The receive array is a uniform linear array (ULA) consisting of 0.4λ separated directional antennas, each having a 3 dB beamwidth of 120°. We can obtain 360° coverage by rotating the array to 3 different positions separated by 120° as depicted in Figure 1. The solid line in Figure 2 depicts one possible realization of the true spectrum, generated with the single-directional SVA model. Given a receive element covariance matrix, how do we estimate directions of arrival?

We may first think of applying a parametric technique such as ESPRIT. Since we have a ULA structure, we can apply

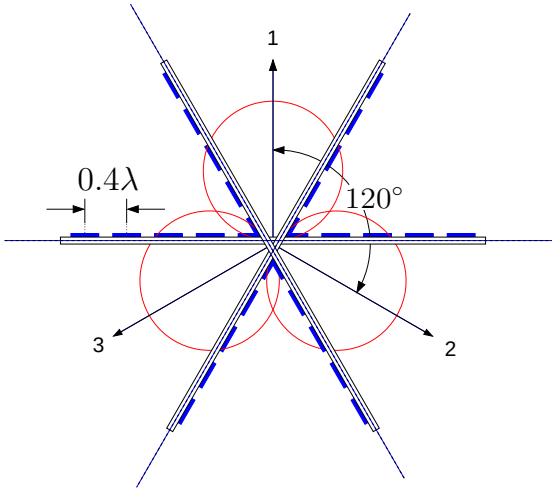

Fig. 1. Directional 8-element array (8 active elements and 2 dummy elements) assuming three possible orientations.

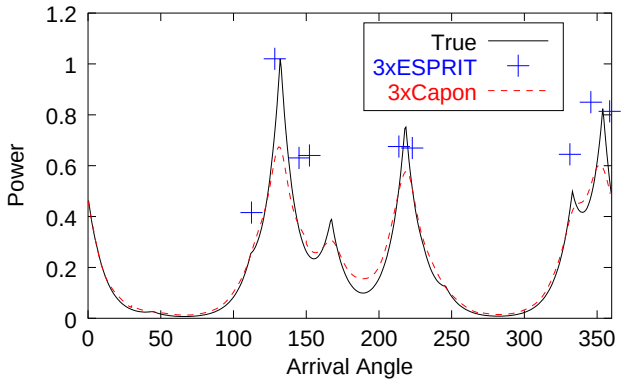

Fig. 2. Example illustrating the difficulty of directional estimation in a diffuse environment.

ESPRIT to each of the three separate orientations. Since the spectrum is diffuse, the model order is very difficult to specify. Simply choosing three arrivals for each look direction, we obtain the crosses in Figure 2, indicating arrival directions and powers. Readily apparent are artifact arrivals and missed weak arrivals, likely due to the violation of ESPRIT's underlying plane wave model.

Another option is to apply a conventional spectral method such as Capon's beamformer, indicated by the dashed line in Figure 2. Here, we apply the beamformer over 120° for each of the three ULA orientations. Encouragingly, Capon's beamformer generates peaks where the true spectral peaks lie. Although the peak smoothing and loss of small peaks with Capon's beamformer may be acceptable, how do we characterize *arrivals* from such a picture? Ideally, we would like to parameterize the spectrum in terms of arrival angles and angular spreads. Since Capon's beamformer only gives an estimate of the spectrum, an additional estimation step would be required to obtain these parameters.

III. Diffuse Spectrum Estimation

The key to this new technique is to assume from the outset that the underlying spectrum is diffuse. That is, the directional channel response is characterized by a continuous power spectrum, and under small-scale fading conditions (small movement or frequency sweep), no permanent phase relationship exists between power propagating in distinct directions. For simplicity, we limit the discussion here to single-directional estimation, although the techniques may be naturally extended to the double-directional case.

A. Relation to Cluster Models

To motivate this diffuse model, let us consider a single-directional version of the SVA model from [5]. The elements of the covariance matrix may be written as

$$R_{mn} = \int_{-\infty}^{\infty} g_m(\theta) g_n^*(\theta) \exp[j\psi_{mn}(\theta)] \underbrace{\sum_{\ell=1}^{L} |\beta_\ell|^2 f(\theta - \theta_\ell)}_{A(\theta)} \, d\theta, \tag{1}$$

where $g_m(\theta)$ is the (complex field) gain pattern of the mth antenna, $\exp(\cdot)$ is an array factor term, L is the number of clusters, $|\beta_\ell|^2$ is the power of the ℓth cluster, and $f(\theta)$ is the probability density function (pdf) of multipath arrival angles within the clusters. The term $A(\theta)$ is the ideal arrival spectrum that would be measured by an array with infinite angular resolution, and this spectrum is diffuse because infinite rays within each cluster were assumed.

B. Problem Definition and LP Solution

In rich-scattering environments, this model is plausible and motivates writing the diffuse spectrum as a sum of power basis functions or

$$A(\theta) = \sum_{i=1}^{N_B} a_i A_i(\theta), \tag{2}$$

where N_B is the number of basis functions, a_i and $A_i(\theta)$ are the power and angular shape associated with the ith basis function. In general, we may have an overcomplete set of basis functions. Substituting $A(\theta)$ into (1), we obtain the relation

$$R_{mn} = \sum_{i=1}^{N_B} a_i \underbrace{\int_{-\infty}^{\infty} A_i(\theta) g_m(\theta) g_n^*(\theta) \exp[j\psi_{mn}(\theta)] \, d\theta}_{Q_{mn,i} = Q_{ki}}. \tag{3}$$

Stacking m and n into a single index $k = m + (n-1)N$, where N is the number of antennas, we obtain the matrix equation $\mathbf{r} = \mathbf{Q}\mathbf{a}$. Since $\mathbf{a}$ is always real, we can split real and imaginary parts of $\mathbf{r}$ and $\mathbf{Q}$ to obtain

$$\begin{bmatrix} \mathbf{r}_R \\ \mathbf{r}_I \end{bmatrix} = \begin{bmatrix} \mathbf{Q}_R \\ \mathbf{Q}_I \end{bmatrix} \mathbf{a}, \tag{4}$$

which may be written as $\mathbf{r}' = \mathbf{Q}'\mathbf{a}$. The obvious way to solve this linear equation is through a simple (pseudo) matrix inverse. Unfortunately, solutions that minimize the 2-norm of $\mathbf{a}$ tend to distribute significant energy into all basis coefficients,

leading to an intractably high model order. Even worse, a simple inverse does not constrain the coefficients (power) to be positive. On the other hand, assuming equality can be achieved, this equation can be solved directly by linear programming (LP). A cost function of $c = \sum_{i=1}^{N_B} a_i$ minimizes the 1-norm of $\mathbf{a}$, favoring a sparse representation [7].

In order to use the method for cluster estimation, we choose a set of basis functions that coincide with all of the cluster arrival angles and shapes we think are possible. For example, Laplacian, Gaussian, and Dirac delta functions might form a reasonable basis. Given a measured $\mathbf{r}$ and known $\mathbf{Q}$, the LP solution returns $\mathbf{a}$, which contains the estimated power in each cluster. The sparse nature of the 1-norm will match the known covariance with only a few basis functions (clusters), thus producing a tractable and intuitive model.

In this development, we have assumed that relation (3) holds exactly. Equality may not be possible due to sources of error such as imperfect estimates of $\mathbf{r}$ or imperfect array calibration. To alleviate this difficulty, we write $\mathbf{r}' = \mathbf{Q}'\mathbf{a} + \boldsymbol{\epsilon}_P - \boldsymbol{\epsilon}_M$ and enforce the bounds $0 \le \epsilon_{Pi} \le \epsilon_i^+$ and $0 \le \epsilon_{Mi} \le \epsilon_i^-$. The cost function then is chosen to minimize both the 1-norm of $\mathbf{a}$ and the absolute error, or $c = c_a \sum_{k=1}^{N_B} a_k + c_\epsilon \sum_{i=1}^{N} (\epsilon_{Pi} + \epsilon_{Mi})$, where c_a and c_ϵ are properly chosen weights. The LP matrix equation in standard form becomes $\mathbf{y} = \mathbf{M}\mathbf{x}$, where

$$\mathbf{y} = \begin{bmatrix} \mathbf{r}' \\ \boldsymbol{\epsilon}^+ \\ \boldsymbol{\epsilon}^- \end{bmatrix} \quad \mathbf{x} = \begin{bmatrix} \mathbf{a} \\ \boldsymbol{\epsilon}_P \\ \boldsymbol{\epsilon}_M \\ \mathbf{p} \\ \mathbf{m} \end{bmatrix} \quad \mathbf{M} = \begin{bmatrix} \mathbf{Q}' & \mathbf{I} & -\mathbf{I} & \mathbf{0} & \mathbf{0} \\ \mathbf{0} & \mathbf{I} & \mathbf{0} & \mathbf{I} & \mathbf{0} \\ \mathbf{0} & \mathbf{0} & \mathbf{I} & \mathbf{0} & \mathbf{I} \end{bmatrix}, \tag{5}$$

p and m are vectors of slack variables, $\mathbf{I}$ is the identity matrix, and $\mathbf{0}$ is the zero matrix.

C. Equation Pruning

We may wish to remove some of the equations in (5), due to redundancy or uncertainty in the covariance matrix. For example, due to shift-invariance, the covariance matrix of a ULA only has a single row or column that is unique. Also, the exact phase relationship between certain antenna elements may be unknown or imprecise. Pruning the vector $\mathbf{r}$ (as well as $\mathbf{y}$ and $\mathbf{M}$) back by removing elements that are either redundant or uncertain reduces the number of equations in (5).

D. Example Application

We demonstrate application of the technique by considering the diffuse spectrum in Section II. Figure 3 depicts the true cluster arrivals (angle/power) and corresponding spectrum with boxes and the solid line, respectively. For diffuse spectrum estimation (DSE), a basis consisting of Laplacian clusters was chosen with angular spreads of $5°, 10°, ..., 35°$ and arrival angles of $0°, 2.5°, ..., 360°$. LP solutions were obtained with the PCx LP solver. DSE arrivals (basis coefficients) and spectrum are plotted as crosses and the dotted line, respectively. Notice that the DSE spectrum is almost exactly the same as the actual spectrum. However, there is quite a discrepancy between the estimated and actual cluster amplitudes and angles. This problem arises because the actual clusters arrive at angles that are between the specified basis functions, and a nonzero coefficient arises on each side. A reduced basis is obtained by only keeping the basis function with the highest power when we have two or more adjacent nonzero basis coefficients. Diffuse spectrum estimation with a reduced basis (DSER) generates cluster arrivals and spectrum shown by X's and the dashed line, respectively. Although the spectrum changes slightly, the cluster parameters are closer to the true values.

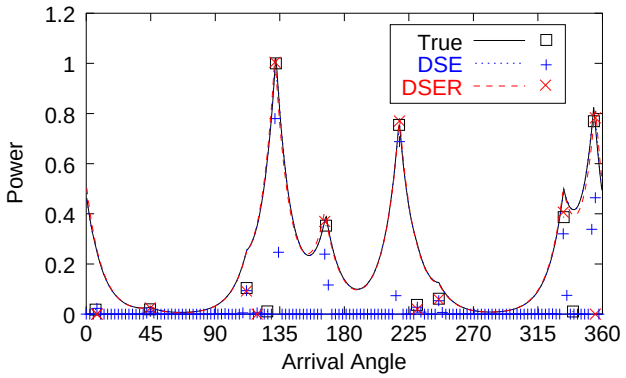

Fig. 3. Example application of diffuse spectrum estimation with a full basis (DSE) and a reduced basis (DSER). Lines represent spectra and symbols represent cluster arrival angle and power.

IV. Application to Measured Data

Now we apply the diffuse spectrum estimation method to measured indoor wireless data at 5.2 GHz, indicating that realistic results can be obtained. Further, we estimate the parameters of the Saleh-Valenzuela angular (SVA) model [5] and compare resulting modeled and measured capacity pdfs.

A. Channel Measurements

Channel matrices were measured in the electrical engineering building on the Vienna University of Technology campus at 5.2 GHz [8]. The transmitter consisted of a positionable monopole antenna on a 20×10 xy grid with $\lambda/2$ inter-element spacing. The receiver employed a directional 8-element ULA provided by T-Systems Nova GmbH, having 0.4λ inter-element spacing and a 3 dB beamwidth of $120°$. The channel was probed at N_F=193 equi-spaced frequency bins covering 120 MHz of bandwidth. The transmitter assumed a single fixed location in a hallway. The receive array assumed many different locations in several offices connected to this hallway, as well as three possible orientations: (1) $0°$ (hallway axis), (2) $-120°$, and (3) $-240°$. The data set for location X and orientation Y is referred to herein as XDY. The transfer coefficient from the jth transmitter to the ith receiver in the kth frequency bin for orientation Y is referred to as $H_{ij}^{(Y,k)}$. For details on the measurements see [4], [8].

Transmit covariance $\mathbf{R}_T^{(Y)}$ and receive covariance $\mathbf{R}_R^{(Y)}$ for

receive orientation Y were computed as

$$R^{(Y)}_{T,j_1 j_2} = \frac{1}{N_F N_R} \sum_{k=1}^{N_F} \sum_{i=1}^{N_R} H^{(Y,k)}_{ij_1} H^{(Y,k)*}_{ij_2} \quad (6)$$

$$R^{(Y)}_{R,i_1 i_2} = \frac{1}{N_F N_T} \sum_{k=1}^{N_F} \sum_{j=1}^{N_T} H^{(Y,k)}_{i_1 j} H^{(Y,k)*}_{i_2 j}, \quad (7)$$

where N_T and N_R are the number of transmit and receive antennas, respectively, and $(\cdot)^*$ is complex conjugate. To allow 360° of angular view at the receiver, a virtual receive array was created by generating a block diagonal covariance matrix $\mathbf{R}_R = \mathrm{diag}(\mathbf{R}_R^{(1)}, \mathbf{R}_R^{(2)}, \mathbf{R}_R^{(3)})$, where $\mathrm{diag}(\cdot)$ creates a block diagonal matrix from its arguments. Setting off block-diagonal elements to zero is fine, since these equations were pruned during estimation. A single transmit covariance matrix $\mathbf{R}_T$ for 360° of view at the receiver was obtained by averaging the three receive orientations, or $\mathbf{R}_T = (1/3)\sum_{Y=1}^{3} \mathbf{R}_T^{(Y)}$.

Since ULAs were involved in the measurement, we improved covariance estimates by enforcing the shift-invariance condition. Specifically, the shift invariant covariance $\mathbf{R}^{\mathrm{SI}}$ is obtained from the standard covariance $\mathbf{R}$ as

$$R^{\mathrm{SI}}_{ij} = \frac{1}{N_{ij}} \sum_{\{\ell,m:\ell-m=i-j\}} R_{\ell m}, \quad (8)$$

where N_{ij} is the number of elements in the sum for the ijth element. After shift invariance is enforced, only a single row of the covariance matrix (per orientation) need be retained.

B. Example Location

Next, we show the performance of the new technique and compare to Capon's beamformer. The basis was the same as in Section III-D. Cluster parameters were estimated separately at transmit and receive to provide better covariance estimates and allow faster convergence of the LP algorithm.

Here, only receive location 9 is considered. For transmit, a 7×7 element cross array (superposition of two 7-element ULAs) was formed. Spatial smoothing was performed in x and y within a 10×10 grid to improve the covariance estimates. For receive, a virtual 24-element array was formed by considering all orientations as a single array and creating a block diagonal covariance matrix as explained in Section IV-A.

Figure 4 compares spectra obtained with DSE and Capon's beamformer for the transmit side. The main discrepancy between Capon's beamformer and the diffuse spectrum estimation techniques occurs in the direction $\theta = 90^\circ$. This artifact appears to be due to aliasing in the endfire directions when element spacing is $\lambda/2$. Thus, the strong energy in the $\theta = 270^\circ$ direction tends to alias into the $\theta = 90^\circ$ direction. Over the range $\theta \in [180^\circ, 360^\circ]$, Capon's beamformer and DSE look similar, with DSE providing a possible resolution enhancement.

Figure 5 shows the comparison at the receive side. Here, Capon's beamformer has been applied separately to the three ULA orientations, and small discontinuities are present. Spectra for Capon's beamformer and DSE/DSER look very similar.

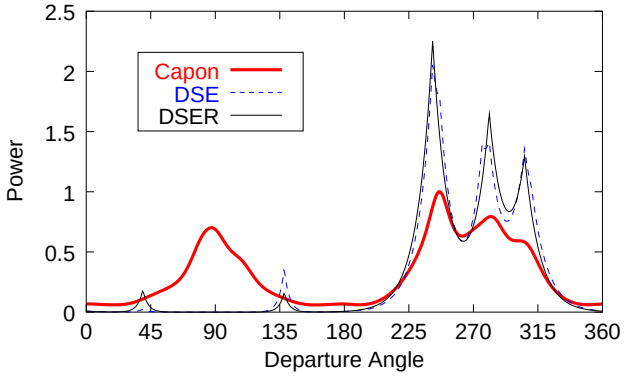

Fig. 4. Estimated transmit spectrum for receive location 9 obtained with Capon's beamformer and diffuse spectrum estimation.

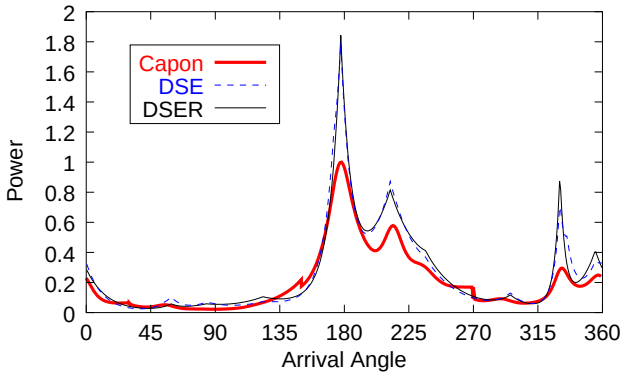

Fig. 5. Estimated receive spectrum for receive location 9 obtained with Capon's beamformer and diffuse spectrum estimation.

C. SVA Model Parameter Extraction

The diffuse spectrum estimation method was applied to measured covariance matrices at all locations to obtain the model cluster parameters in exactly the same manner as the previous example. The key parameters to be obtained from the estimated clusters are the distribution on cluster departure and arrival angle, cluster decay constant (Γ), and cluster angular spread at transmit (σ_T) and receive (σ_R). Cluster departure angle at the transmitter was found to favor propagation down the hallway, and was approximated with a pdf proportional to $|\cos(\theta)|$, with 0° as the axis of the hallway. Cluster arrival angle appeared to have little directional preference, and was approximated with a uniform distribution. A simple average was taken of the cluster angular spread at transmit and receive to obtain $\sigma_T = 11^\circ$ and $\sigma_R = 17^\circ$. The cluster decay constant was obtained by considering the three strongest clusters for each location and applying maximum likelihood assuming the Poisson arrival process with unit arrival rate and exponential cluster decay, resulting in $\Gamma = 1.5$.

D. Capacity pdf Comparisons

To show the plausibility of the extracted SVA model parameters, Figure 6 compares the capacity pdfs for an 8×8 MIMO system computed from the measured data (see [8]) and 5×10^4 random realizations of the SVA model. Here capacity was

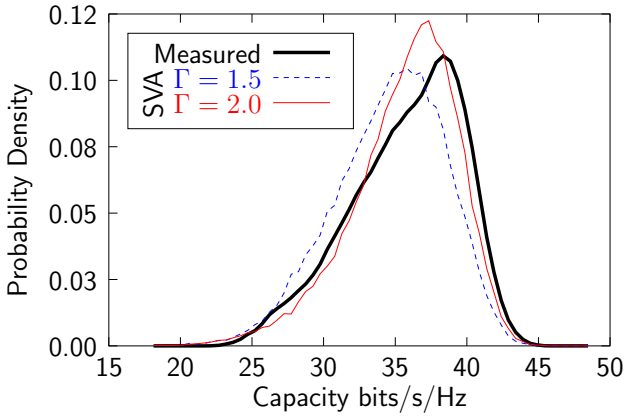

Fig. 6. Capacity pdf of all measured channels and those synthesized with the SVA model.

computed with the water-filling solution assuming an average SISO SNR of 20 dB. To improve the capacity fit, the decay constant Γ was increased to 2.0. One of the problems with estimating Γ is that the SVA model generates overlapping clusters, which often look like a single cluster. However, if two clusters were to overlap in the data, the diffuse estimation technique would likely only find a single cluster. Therefore, this estimation method tends to underestimate Γ and the needed increase is not surprising.

Finally, to demonstrate that the SVA model produces more realistic channel realizations than convenient correlation functions (Jakes' model, exponential, etc.), Figure 7 plots the joint Fourier spectrum [3], [4] of the 8×8 channel matrix data for location 9D1. Also plotted is the joint spectrum of a single realization of the SVA model with the parameters found above and Jakes' model. Note here that we are not expecting agreement in the various joint spectra, but rather qualitative agreement in the number of arrival clusters, cluster shape, etc. Jakes' model tends to over-estimate the multipath richness, as indicated in the plot where significant power is communicated from all transmit directions to all receive directions. The random realization of the SVA model, on the other hand, looks qualitatively more like spectra obtained from measured channels. Only a few paths, or arrival/departure clusters, support power transfer through the channel.

V. Conclusion

This paper has presented a new direction-finding technique for diffuse multipath channels. Such channels occur in practice due to rough-surface scattering mechanisms or channel probing hardware with limited temporal and spatial discrimination. When the underlying channel is diffuse, parametric methods (such as ESPRIT) do not produce accurate results. Although beamforming methods may produce acceptable estimates of the true spectrum, structure such as multipath clustering is hidden. We have presented a new diffuse spectrum estimation method that reveals cluster parameters through proper basis function selection and a linear programming solution. Application of the method to indoor measured radio channels

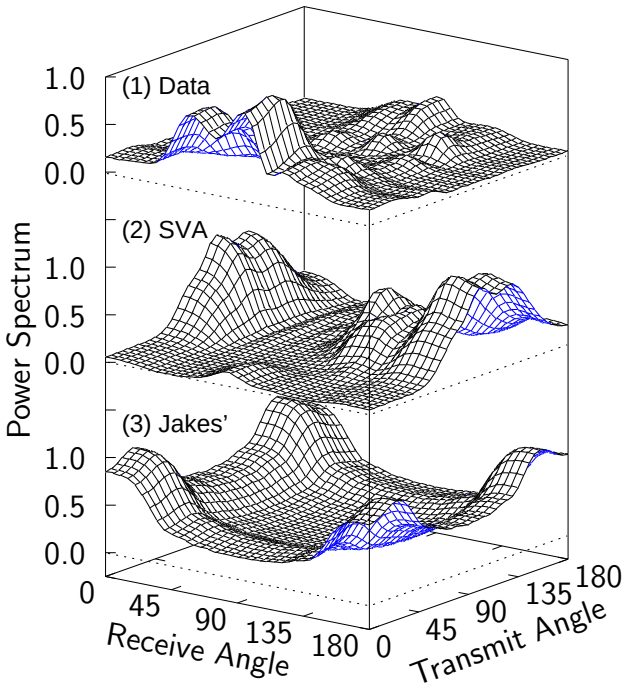

Fig. 7. Joint transmit/receive spectra for (1) data location 9D1, (2) a random realization of the SVA model, and (3) Jakes' model.

at 5.2 GHz demonstrated the direction-finding capabilities of the method. We used the method to obtain parameters for a path-based channel model. Capacity pdfs of measured data and synthetic channels generated with the resulting model exhibited good agreement. The new method holds promise for double-directional MIMO channel modeling in very rich scattering environments, such as the indoor wireless channel.

References

[1] M. Steinbauer, A. F. Molisch, and E. Bonek, "The double-directional radio channel," *IEEE Antennas and Propagation Magazine*, vol. 43, pp. 51–63, Aug. 2001.

[2] A. Richter, D. Hampicke, G. Sommerkorn, and R. S. Thoma, "Joint estimation of DoD, time-delay, and DoA for high-resolution channel sounding," in *IEEE VTC'2000 Spring Conf.*, Tokyo, Japan, May 15-18 2000, vol. 2, pp. 1045–1049.

[3] H. Krim and M. Viberg, "Two decades of array signal processing research: the parametric approach," *IEEE Signal Processing Magazine*, vol. 13, pp. 67–94, July 1996.

[4] J. Wallace, H. Özcelik, M. Herdin, E. Bonek, and M. Jensen, "Power and complex envelope correlation for modeling measured indoor MIMO channels: A beamforming evaluation," in *IEEE VTC'2003 Fall Conf.*, Orlando, Florida, Oct. 6-10 2003.

[5] J. W. Wallace and M. A. Jensen, "Modeling the indoor MIMO wireless channel," *IEEE Transactions on Antennas and Propagation*, vol. 50, pp. 591–599, May 2002.

[6] Q. H. Spencer, B. D. Jeffs, M. A. Jensen, and A. L. Swindlehurst, "Modeling the statistical time and angle of arrival characteristics of an indoor multipath channel," *IEEE Journal on Selected Areas in Communications*, vol. 18, pp. 347–360, Mar. 2000.

[7] S. S. Chen, D. L. Donoho, and M. A. Saunders, "Atomic decomposition by basis pursuit," *SIAM Review*, vol. 43, pp. 129–159, Mar. 2001.

[8] M. Herdin, H. Ozcelik, H. Hofstetter, and E. Bonek, "Variation of measured indoor MIMO capacity with receive direction and position at 5.2 GHz," *Electronics Letters*, vol. 38, pp. 1283–1285, Oct. 10, 2002.